Polymer 50 (2009) 756–766

Contents lists available at ScienceDirect

Polymer

journal homepage: www.elsevier.com/locate/polymer

PEG-based hydrogel membrane coatings

Alyson C. Sagle [a], Hao Ju [a], Benny D. Freeman [a,*], Mukul M. Sharma [b]

[a] University of Texas at Austin, Center for Energy and Environmental Resources, 10100 Burnet Road, Building 133, Austin TX 78758, United States
[b] University of Texas at Austin, Department of Petroleum and Geosystems Engineering, 1 University Station C0300, Austin TX 78712, United States

ARTICLE INFO

Article history:
Received 22 September 2008
Received in revised form
8 December 2008
Accepted 9 December 2008
Available online 14 December 2008

Keywords:
Hydrogel
Poly(ethylene glycol) diacrylate
Water permeability

ABSTRACT

As a first step towards preparing fouling-resistant coatings for water purification membranes, three series of copolymer hydrogel networks were synthesized using poly(ethylene glycol) diacrylate (PEGDA) as the crosslinker and acrylic acid (AA), 2-hydroxyethyl acrylate (HEA), or poly(ethylene glycol) acrylate (PEGA) as comonomers. Copolymers containing varying amounts of PEGDA with each of these comonomers were prepared. Glass transition temperatures obeyed the Fox equation. Crosslink density strongly influenced water uptake and water permeability for materials of constant chemical composition. For example, the volume fraction of water sorbed by a 100 mol% PEGDA hydrogel was 0.61. However, introducing comonomers into the network reduced hydrogel crosslink density, and in hydrogels having the same ethylene oxide content, water sorption increased as crosslink density decreased. The highest water volume fraction observed was 0.72, obtained in a copolymer containing 80 mol% PEGA and 20 mol% PEGDA. Water permeability increased systematically with increasing water sorption, and water permeability coefficients ranged from 10 to 26 L μm/(m^2 h bar). NaCl partition coefficients ranged from 0.36 to 0.53 (g NaCl/cm^3 hydrogel)/(g NaCl/cm^3 solution). NaCl diffusion coefficients varied little with polymer composition; in this regard, diffusion coefficient values ranged from 4.3×10^{-6} to 7.4×10^{-6} cm^2/s. Based on contact angle measurements using *n*-decane in water, oil exhibited a low affinity for the surfaces of these polymers, suggesting that coatings prepared from such materials might improve the fouling resistance of membranes towards oily wastewater.

1. Introduction

The search for new water resources continues as demand for fresh water increases worldwide [1]. One potential resource is produced water, a byproduct of oil and natural gas production, which is a complex emulsion composed of oil and other organics, salts, and particulate matter [2]. An estimated 77 billion barrels of produced water are generated worldwide each year [2]. Currently, 92% of produced water is reinjected, but cost-effective treatment could provide new water sources for beneficial uses in applications such as irrigation, power generation, and even human consumption [2].

Reverse osmosis (RO) membranes could potentially be used to purify produced water. RO membranes are capable of removing up to 99.9% of monovalent salts as well as particulates and emulsified oil [3]. However, RO membranes foul strongly in the presence of oily feed waters [4]. Fouling occurs when oil droplets or other contaminants are deposited on the surface of the membrane, causing a sharp decline in water flux. One proposed solution to reduce membrane fouling by oily wastewater is to apply a hydrophilic coating to the membrane surface [4,5]. An ideal coating would be hydrophilic, resist oil droplet adhesion, and minimally impact the water flux and salt rejection of the underlying desalination membrane.

Hydrophilic membrane coating materials synthesized from poly(ethylene glycol) (PEG)-based hydrogels are the focus of this study. Hydrogel materials are crosslinked polymer networks with a high affinity for water; they swell significantly in water, but do not dissolve in it [6]. More specifically, PEG-based hydrogels are versatile materials that are highly hydrophilic, readily chemically modified, and biocompatible [7]. Such materials derive their high hydrophilicity from the ethylene oxide linkages in the polymer backbone [7]. Unmodified PEG chains are soluble in water, but crosslinking renders them insoluble. Chemical modification of PEG chain ends facilitates crosslinking [6]. For example, the chain ends can be terminated with acrylate groups, which can then crosslink via polymerization [7].

Some of the material design strategies employed in this work are derived from studies aimed at reducing the adhesion of proteins to surfaces. Like emulsified oil droplets, proteins can be strong

* Corresponding author. Tel.: +1 512 232 2803; fax: +1 512 232 2807.
E-mail address: freeman@che.utexas.edu (B.D. Freeman).

0032-3861/$ – see front matter © 2008 Elsevier Ltd. All rights reserved.
doi:10.1016/j.polymer.2008.12.019

foulants for membranes [8]. However, many proteins such as lysozyme and human serum proteins adhere poorly to surfaces rich in PEG segments [9,10]. Furthermore, the molecular structural details of the PEG moieties, such as the length of PEG brushes on the surface and PEG brush chain density, have been correlated with the extent of protein adhesion resistance. High densities of short chains as well as lower densities of longer PEG chains were effective in reducing protein adsorption [9,10].

The goal of this study is to explore fundamental relationships between copolymer structure and hydrogel properties in potential fouling-resistant coating materials. In this regard, three series of copolymer hydrogels were synthesized using comonomers of varying chain lengths. In addition to fundamental polymer characterization, water and NaCl transport properties of the copolymers were measured and correlated with copolymer structure. This study of PEG-containing hydrogels complements recent work showing the efficacy of such hydrogel materials for reducing fouling of coated ultrafiltration membranes by oil/water emulsions [5].

2. Experimental

2.1. Materials

The crosslinker, poly(ethylene glycol) diacrylate (PEGDA: MW = 698, $n = 13$), and the monomers, poly(ethylene glycol) acrylate (PEGA: MW = 380 g/mol, $n = 7$), 2-hydroxyethyl acrylate (HEA: MW = 116 g/mol, $n = 1$), and acrylic acid (AA: MW = 72 g/mol) were obtained from Sigma–Aldrich. Previous work carefully characterized PEGDA and PEGA as received from the manufacturer and found the materials to have a narrow molecular weight distribution [11,12]. Thus, PEGDA and PEGA were used without further purification in this study. AA was purified using vacuum distillation [13–15], and the product purity was confirmed using ^{1}H NMR. Water uptake was measured in hydrogels synthesized with distilled AA and those prepared with as-received AA. There was no significant difference in water uptake between the samples prepared from distilled AA and as-received AA, suggesting that the properties of interest for this study are not materially affected by this additional purification step. Subsequently, for the data presented in this study, AA was used as received, without further purification. HEA was also used without further purification. The photoinitiator was 1-hydroxycyclohexyl phenyl ketone (HPK), which was also obtained from Sigma–Aldrich and used as received.

These three monomers, PEGA, HEA, and AA, were chosen to systematically study the influence of comonomer chain length (i.e., the number of ethylene oxide (EO) units in the pendant chain), and subsequently, poly(ethylene oxide) (PEO) content, on material properties. The structures of these components are presented in Fig. 1. Each monomer has an acrylic endgroup and a hydroxyl endgroup. However, AA does not contain any EO, HEA contains one EO unit, and PEGA contains seven EO units.

Table 1
Composition of copolymers.

Sample	Mol% comonomer	wt% comonomer	wt% Poly(ethylene oxide)
PEGDA	0	0	82
20AA	20	2.5	80
40AA	40	6.4	77
60AA	60	13	71
80AA	80	29	58
20HEA	20	4.0	80
40HEA	40	10	78
60HEA	60	20	73
80HEA	80	40	64
20PEGA	20	12	82
40PEGA	40	26	82
60PEGA	60	45	82
80PEGA	80	68	81

2.2. Hydrogel synthesis

Prepolymerization mixtures were prepared by combining desired amounts of crosslinker and monomer on a molar basis with a specified amount of deionized (DI) water and 1.0 wt% (based on total crosslinker and monomer contents) of photoinitiator. The crosslinker, monomer, and photoinitiator were first mixed in an amber glass jar and stirred with a magnetic stir bar for approximately 1 h to completely dissolve the photoinitiator. An amber glass jar was used to minimize solution exposure to light. After the photoinitiator dissolved, the appropriate amount of DI water was added, and the solution was stirred for an additional hour. DI water was taken from a Millipore MilliQ system (18.2 MΩ-cm, 1.2 ppb). In this study, the water content in the prepolymerization mixture was 60 wt%, based on total mixture weight. This water content was chosen because previous studies found that 60 wt% H_2O produced highly permeable and mechanically strong hydrogels [5]. Above 60 wt% H_2O, the hydrogels became increasingly fragile and were often phase-separated [5]. The films were named based on monomer content and monomer type. For example, a "60PEGA" film was polymerized from a mixture containing 60 mol% PEGA and 40 mol% PEGDA. In all the cases, the monomer and crosslinker together comprised 40 wt% of the total prepolymerization solution, and the remaining 60 wt% of the prepolymerization solution was water. Table 1 presents a summary of the composition, on a dry basis, of hydrogels prepared for this study.

Dense free-standing films were prepared by first placing the prepolymerization mixture between two quartz plates, using two feeler gauges as spacers (Stanley-Proto Industrial Tools, New Britain, CT) to control film thickness. Then, the mixture was exposed to

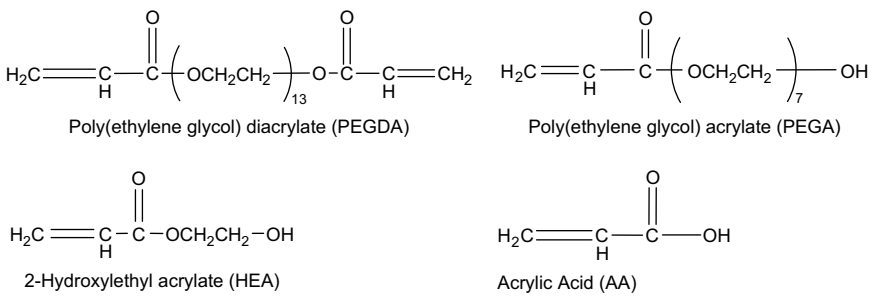

Fig. 1. Chemical structures of hydrogel components.

312 nm wavelength UV-light for 90 s at 3000 μW/cm^2 in a Fisher-Scientific UV-Crosslinking chamber (Pittsburgh, PA). Films were removed from the quartz plates, rinsed, and soaked in DI water until used. Sol fractions in the hydrogels were found to be negligible based on a 5 day extraction in water. This result is consistent with previous studies on similar copolymer materials [12]. Therefore, no further extraction was performed apart from rinsing and storing the polymerized films in DI water.

2.3. ATR-FTIR

Attenuated total reflection Fourier transform infrared spectroscopy (ATR-FTIR) was performed using a Thermo Nicolet Nexus 470 FTIR (Madison, WI) with an Avatar Smart MIRacle ATR accessory (Zinc Selenide crystal). Data were collected and analyzed using Omnic software. Spectra were collected using 128 scans at a resolution of 4 cm^{-1} between 600 and 4000 cm^{-1}. Prior to analysis, samples were placed under vacuum overnight at room temperature to remove water.

ATR-FTIR was used to gauge reaction conversion of the hydrogels. Sharp peaks at 810, 1190, and 1410 cm^{-1} result from vibrations of the unreacted CdbndC bond in the acrylate endgroups; disappearance of these peaks indicates that the acrylate groups have reacted [12,16–19].

2.4. Density and thermal characterization

Dry film density was determined via hydrostatic weighing, using a Mettler Toledo analytical balance (Model AG 204) and a Mettler Toledo density determination kit (Part # 238490). Film density, ρ_p, was calculated as follows:

$$\rho_p = \frac{M_A}{M_A - M_L}\rho_0 \tag{1}$$

where M_A is the film weight measured in air, M_L is the film weight measured in a non-solvent (i.e., a liquid that does not swell the polymer), and ρ_0 is the density of the non-solvent. Hexane was used as the non-solvent after hexane uptake by the materials was found to be negligible, consistent with previous results on similar materials [11]. All films were dried under vacuum overnight at room temperature prior to measurement.

Differential scanning calorimetry (DSC) was performed using a TA Instruments Q100 (New Castle, DE). Samples were dried overnight under vacuum at room temperature prior to testing. Samples were heated to 150 °C at 10 °C/min, held for 5 min, and then cooled to −80 °C at 5 °C/min. This cycle was repeated, and the second cycle was used for analysis. The data were analyzed using the Universal Analysis 2000 software provided by TA instruments. The glass transition temperature, T_g, was taken as the midpoint of the heat capacity step change. The T_g values were compared to predictions by the Fox equation [20]:

$$\frac{1}{T_g} = \frac{w_{PEGDA}}{T_{gPEGDA}} + \frac{w_{Monomer}}{T_{gMonomer}} \tag{2}$$

where w_{PEGDA} and $w_{Monomer}$ are the weight fractions of PEGDA and monomer in the final polymerized copolymer, respectively. T_{gPEGDA} is the T_g of polymerized pure PEGDA, and $T_{gMonomer}$ is the T_g of polymerized pure comonomer.

2.5. Water transport properties

Water uptake in free-standing hydrogel films was measured gravimetrically. Films were equilibrated in DI water for a minimum of1 h. The films were then patted dry with a tissue and quickly weighed using an analytical balance. Afterwards, the samples were dried overnight under vacuum at room temperature and weighed again. This process was repeated until changes in each measured weight were less than 1 wt%. The volume fraction of water in the swollen network, ν_{H_2O}, was calculated assuming ideal mixing behavior [21,22]:

$$\nu_{H_2O} = \frac{\frac{m_{wet} - m_{dry}}{\rho_{H_2O}}}{\frac{m_{wet} - m_{dry}}{\rho_{H_2O}} + \frac{m_{dry}}{\rho_p}} \tag{3}$$

where m_{wet} is the mass of the wet film, m_{dry} is the mass of the dry film, ρ_{H_2O} is the density of water, and ρ_p is the measured polymer density. Water volume fraction was directly measured for a few representative samples following the method outlined by Peppas and Barr-Howell, which is based on Archimedes' buoyancy principle [23]. The measured water volume fraction was equal, within experimental error, to the volume fraction calculated using hydrogel water uptake, dry (i.e., not hydrated) polymer density, and Eq. (3). Therefore Eq. (3) is assumed to be valid for the materials considered in this study.

Water uptake values at activities less than one were measured using a salt solution in a desiccator [24]. Hydrogels were placed on a tray in a desiccator above a 5 wt% NaCl solution at ambient temperature and pressure. Under these conditions, the activity of water in a 5 wt% NaCl solution is 0.97 [25]. The desiccator was sealed using a vacuum pump, and samples were allowed to equilibrate with the water vapor for 24 h before measurement. Mass was measured daily until changes were less than 1 wt%. Then, samples were dried overnight under vacuum and weighed to determine the dry mass.

Hydrogel water flux was measured using dead-end filtration. Advantec MFS, Inc. UHP 43 (diameter 43 mm) dead-end filtration cells (Dublin, CA) were used at upstream pressures ranging from 1.7 to 4.5 bar (10–50 psig) and 25 °C. The downstream pressure was always atmospheric. Permeate volume, V, as a function of time, t, was recorded, and the steady-state water flux, J_{H_2O}, was calculated as follows:

$$J_{H_2O} = \frac{\Delta V}{\Delta t}\frac{1}{A} \tag{4}$$

where A is the active hydrogel area. Then, water flux was used to calculate water permeability, P_{H_2O}:

$$P_{H_2O} = \frac{J_{H_2O} l}{\Delta p} \tag{5}$$

where l is the film thickness of a hydrated film, and Δp is the applied transmembrane pressure difference.

Ultrapure water from a Millipore MilliQ system (18.2 MΩ-cm, 1.2 ppb) was used in all sorption and permeation experiments. Film thickness was measured using a Mitutoyo Absolute micrometer (Model ID-C112E, Mitutoyo USA, Aurora, IL) following ISO 9339-2 [26]. Water flux was measured at a minimum of three different upstream pressures, and a plot was made of water permeability as a function of applied pressure. The reported water permeability was the average of the individual permeabilities.

2.6. Salt transport properties

Salt transport in hydrogel films was evaluated using kinetic desorption experiments [27,28]. A hydrogel film was immersed in 50 cm^3 of 5 wt% NaCl (0.86 M). After 24 h, the film was removed and quickly patted dry. Then, the film was placed in a beaker containing 50 cm^3 of DI water, and the beaker was sealed with

Parafilm to minimize changes in solution conductivity due to CO_2 absorption by the water. The solution was stirred at approximately 300 rpm to ensure a uniform salt concentration in the beaker. Solution conductivity was measured as a function of time at 25 °C using an InoLab WTW 730 Conductivity meter (WTW, Woburn, MA), and the data were recorded at 5 s intervals. Conductivity was converted to NaCl concentration using a calibration curve.

The diffusion coefficient of NaCl in the hydrogel film was calculated based on a Fickian analysis of solute desorption from a planar film [27,29]. M_t/M_∞ was plotted versus $t^{1/2}$, where M_t is the mass of salt in the water solution at time t (i.e., the mass of salt desorbed from the hydrogel), and M_∞ is the total amount of salt desorbed from the polymer into the solution. For $M_t/M_\infty < 0.6$, M_t/M_∞ should be a linear function of $t^{1/2}$, and the diffusion coefficient, D_s, is calculated as follows [27]:

$$D_s = \frac{\pi l^2}{16}\left[\frac{d(M_t/M_\infty)}{d(t^{1/2})}\right]^2 \quad (6)$$

where $d(M_t/M_\infty)/d(t^{1/2})$ is the slope in the linear region of a plot of M_t/M_∞ versus $t^{1/2}$, and l is the thickness of the hydrated film.

The salt partition coefficient, K_s, is the ratio of the mass of NaCl in the polymer, M_∞, per unit hydrogel volume, to the concentration of NaCl in the original solution (i.e., NaCl/cm^3 hydrogel/g Nacl/cm^3 solution). The salt permeability coefficient, P_s, was estimated from the measured diffusion and partition coefficients [28]:

$$P_s = D_s K_s \quad (7)$$

2.7. Contact angles

A Ramé-Hart NRL contact angle goniometer (Model 100, Ramé-Hart Instrument Co., Mountain Lakes, NJ) with an environmental chamber was used to conduct pendant drop contact angle measurements. The environmental chamber was filled with DI water, and the probe liquid was *n*-decane. *n*-Decane was chosen because of its immiscibility with water, and because it is a straight-chain hydrocarbon representative of alkyl hydrocarbons in produced water [2]. A minimum of three drops were measured, and the drop volume was approximately 1 μL for each sample measurement.

3. Results and discussion

3.1. Hydrogel synthesis

Hydrogel films were synthesized using the crosslinker, PEGDA, and either PEGA, HEA, or AA as the comonomer. All prepolymer mixtures were visually transparent and homogeneous. All of the polymerized films, except for 80AA, were optically clear, had good mechanical integrity, and therefore, were assumed to be nonporous. However, even though the 80AA prepolymer mixture was transparent, the 80AA film was milky-colored, characteristic of a phase-separated material [30]. Phase-separated materials may have a macroporous structure [30], so the 80AA copolymer was not presumed to be nonporous.

Reaction conversion was gauged used ATR-FTIR [11,16–19]. The FTIR spectrum of 100PEGDA matches with that previously reported in the literature [11]. Analysis of each copolymer spectrum reveals the disappearance of the acrylate-associated peaks of the comonomers, indicating double bond conversion. Fig. 2a presents representative FTIR-ATR spectra of the AA monomer, a polymerized PEGDA film, and an 80AA copolymer film (i.e., 80 mol% AA and 20 mol% PEGDA). These spectra clearly show the disappearance of the acrylate peaks in the polymerized films. The results in Fig. 2a are representative of results obtained from all other copolymers considered in this study.

During photopolymerization, the top of a film is closer to the UV source than the bottom of the film. Therefore, the top surface would receive a higher dose of UV radiation than the bottom of the film, potentially resulting in differences in the extent of polymerization as a function of depth through the sample. This effect could be further exacerbated by polymerizing an extremely thick film. To gauge the potential changes in reaction conversion due to film thickness, ATR-FTIR spectra for 80HEA films of two different thicknesses were taken (cf., Fig. 2b), and the differences between the two spectra were calculated. Based on the lack of appreciable differences between these spectra, there is no detectable influence of film thickness on conversion over the range of film thicknesses considered. To further insure that the reaction conversion was independent of film thickness, two prepolymerization solutions were placed, in a sandwich-like stacked arrangement between three quartz plates and photopolymerized using the parameters noted earlier. In this way, the UV radiation that polymerized the bottom sample was obliged to first pass through a polymerizing mixture of equal thickness and two quartz plates. Then, these thick (700 μm thick) polymerized films were analyzed using ATR-FTIR. Fig. 2c presents the spectra of these two thick films and the subtraction spectrum between them. Because the two spectra are essentially identical, there is no detectable difference in conversion between these two films. Therefore, thick films in this study are presumed to be homogeneous and completely polymerized.

3.2. Physical characterization

Film density and thermal properties were evaluated to determine the influence of comonomer pendant chain length on these fundamental polymer properties. As shown in Fig. 3a, the density of dry (i.e., not hydrated) films increases with increasing AA and HEA contents, but density is essentially unchanged for PEGA copolymers. Each comonomer (i.e., AA, HEA, and PEGA) has a hydroxyl endgroup available for hydrogen bonding. Increasing the number of hydrogen bonding moieties in a material should increase the attractive intermolecular interactions in the material and, therefore, contribute to a denser network structure [22]. However, the tendency towards a denser structure because of hydrogen bonding may be counterbalanced by the increase of pendant chains in the hydrogel network, which can disrupt polymer chain packing [31]. AA does not introduce a long pendant chain to the PEGDA network, so AA copolymers are more strongly influenced by additional hydrogen bonding than HEA and PEGA copolymers. Consequently, the density of the resulting AA copolymer films increases systematically with increasing AA content. HEA is bulkier than AA because of the ethylene oxide unit in HEA. Therefore, HEA copolymers exhibit lower density than AA copolymers at the same comonomer content. PEGA is bulkier than both AA and HEA because PEGA has seven EO units in its chain. As a result, PEGA copolymers have the lowest density at a given concentration of comonomer.

The density data in Fig. 3a are presented as specific volume versus comonomer weight percent in Fig. 3b. The specific volumes of the pure polymerized monomers were measured and used, along with an ideal mixing model, to predict copolymer specific volume [32]:

$$\hat{V}_p = w_{PEGDA}\hat{V}_{PEGDA} + w_{Monomer}\hat{V}_{Monomer} \quad (8)$$

where $\hat{V}_p$, $\hat{V}_{PEGDA}$, and $\hat{V}_{Monomer}$ are the specific volumes of the copolymer, polymerized PEGDA, and polymerized comonomer, respectively, and w_{PEGDA} and $w_{Monomer}$ are the weight fractions of

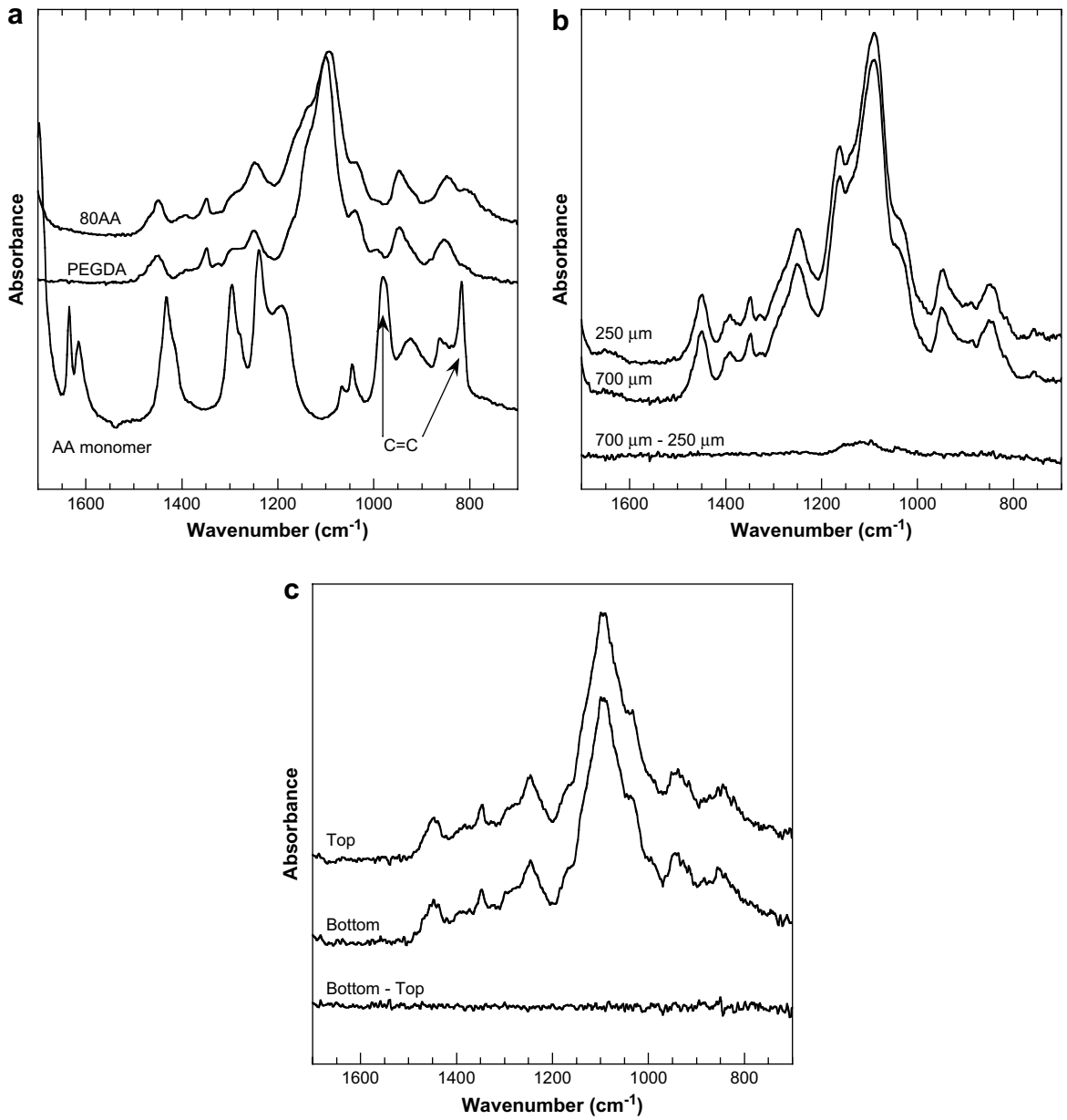

Fig. 2. FTIR spectra of (a) crosslinked PEGDA, 80AA film and AA monomer. The PEGDA and 80AA films were approximately 250 μm thick. (b) Two 80HEA films of different thicknesses and the subtraction spectrum between them, and (c) two 700 μm 80PEGA films which were placed in a sandwich arrangement separated by quartz plates and polymerized one on top of the other and the subtraction spectrum between them. The spectra have been displaced vertically for easier viewing.

PEGDA and comonomer, respectively. These weight fractions are based on the amount of PEGDA and comonomer in the polymerization mixture and do not include contributions from the water and photoinitiator also present in the polymerization mixture.

Comparing calculated specific volume to measured specific volume values sheds light on possible polymer interactions [33]. In this regard, the solid lines in Fig. 3b represent Eq. (8) with the parameters coming from independent measurements of the density of pure polymerized PEGDA and pure polymerized PEGA, HEA, and AA and the appropriate weight fractions. If copolymers follow ideal mixing behavior, then the resulting copolymer specific volume should closely obey Eq. (8). This behavior is observed with the HEA and PEGA copolymers; the experimental specific volumes for HEA and PEGA copolymers agree well with Eq. (8). However, deviations from ideal mixing behavior can indicate the occurrence of additional intermolecular interactions [32]. Such deviations are observed with AA copolymers; the experimental specific volumes are somewhat lower than the predicted specific volumes. This negative deviation from Eq. (8) suggests the presence of attractive polymer–polymer interactions such as hydrogen bonding within AA copolymers, which would serve to induce denser chain packing and therefore, lower specific volume [33]. In support of this interpretation, AA is known to participate extensively in hydrogen bonding through its hydroxyl and carbonyl chemical moieties [34,35].

Fig. 4 presents glass transition temperature (T_g) data for dry copolymer films. A single T_g was observed for each copolymer, indicating that these materials are random copolymers [20]. It was anticipated that these copolymers would be random, because many similar acrylate systems have reactivity ratios close to one [36], and

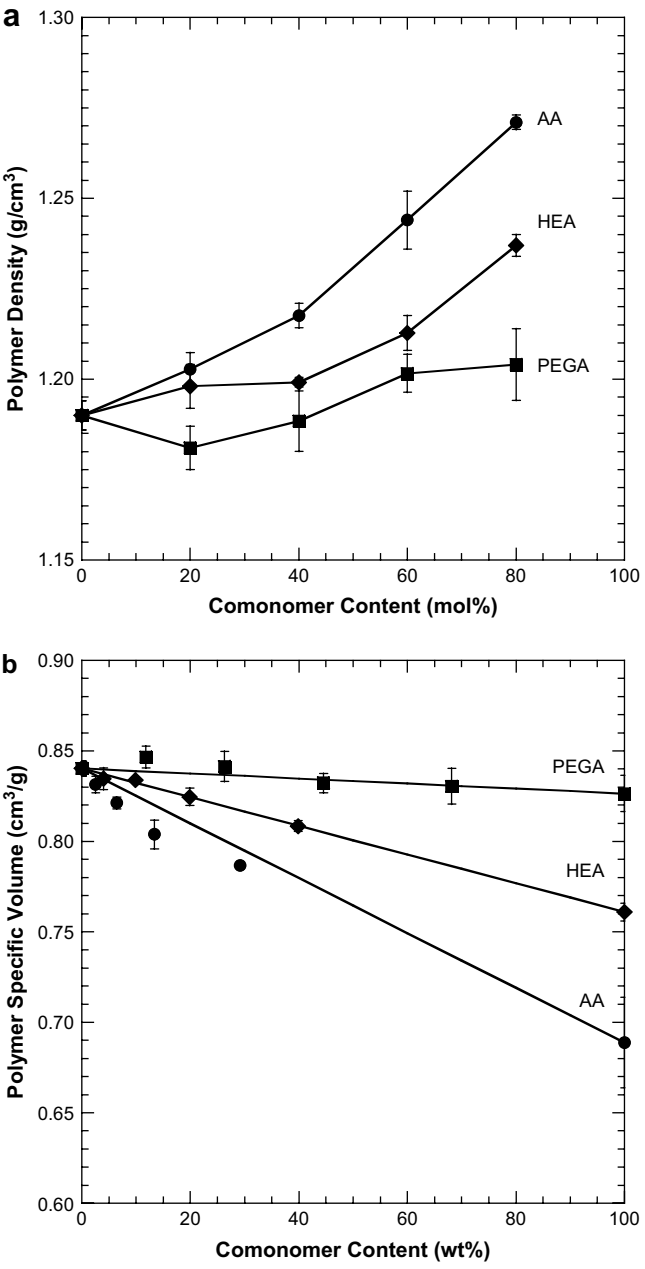

Fig. 3. (a) Dry film density as a function of comonomer composition, and (b) Dry polymer specific volume as a function of comonomer weight %. Solid lines represent specific volume predicted by the ideal volume additivity model [32].

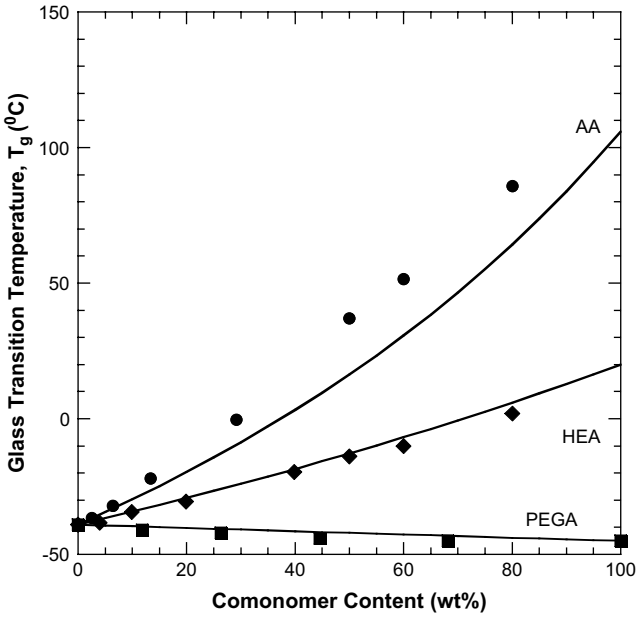

Fig. 4. Effect of copolymer composition on glass transition temperature of AA, HEA, and PEGA copolymers. Solid lines correspond to the predictions of the Fox equation (Eq. (2)). The following T_g values were used in the Fox equation: $T_{gPEGDA} = -39\,^{\circ}C$ [12], $T_{gAA} = 106\,^{\circ}C$ [37], $T_{gHEA} = 20\,^{\circ}C$ [38], and $T_{gPEGA} = -45\,^{\circ}C$ [12].

are, therefore, random copolymers. The PEGDA T_g measured in this work matches the previously published value [12]. Literature T_g values for 100AA [37], 100HEA [38], and 100PEGA [12] were used along with the T_g of PEGDA and the Fox equation, Eq. (2), to predict copolymer T_g values. Measured T_g values of HEA and PEGA copolymers in this study closely match literature values [12,39] and also values predicted by the Fox equation, further supporting the random nature of the copolymers. Measured T_g values for AA copolymers are higher than the predicted values. One possible explanation is the wide range of T_g values presented in the literature for polyacrylic acid (100AA) [37], due in part to the highly reactive nature of the material. Anhydrides form as 100AA is heated, increasing the T_g [37] and making it difficult to accurately measure one T_g for 100AA. Attempts to measure the T_g of 100AA in this study encountered similar difficulties. Therefore, the literature T_g value that most closely matched the measured value was used in Eq. (2). This choice in 100AA T_g could explain the disagreement between the measured AA copolymer T_g values and the predicted T_g values. Another possibility is the presence of hydrogen bonding in the AA copolymers, already seen to influence copolymer specific volume. Increased hydrogen bonding can result in lower copolymer chain mobility, and subsequently, higher T_g values [39].

DSC scans did not show any discernable crystallinity, indicating that the hydrogels are completely amorphous. Such amorphous rubbers are desired for this application because they are expected to be much more permeable to water than semicrystalline materials [40].

3.3. Water sorption and transport properties

Fig. 5a presents water sorption (i.e., equilibrium volume fraction of sorbed water) measured in pure water and in a vapor environment where the water activity was 0.97, which corresponds to the activity of water in a 5 wt% solution of NaCl. PEGA copolymers exhibit the highest water uptake, and water uptake increases systematically as PEGA content increases. HEA copolymers sorb more water than a pure PEGDA hydrogel, but show little change in water uptake with comonomer content. The water volume fraction in AA copolymers is, at most, only slightly higher than that of PEGDA, but changes little with comonomer content. For all materials, water sorption is lower at lower water activity, as expected [6].

The observed water sorption behavior presumably stems from the monomer chemistry and crosslink density of each copolymer. Fig. 5a clearly shows the influence of comonomer type on the copolymer water sorption. In general, water sorption increases with increasing comonomer chain length. For example, at 60 mol% comonomer, the lowest copolymer water uptake corresponds to the copolymer with the shortest chain, 60AA, and the highest water uptake corresponds to the copolymer with the longest chain, 60PEGA. Subsequently, the copolymer with the mid-length chain,

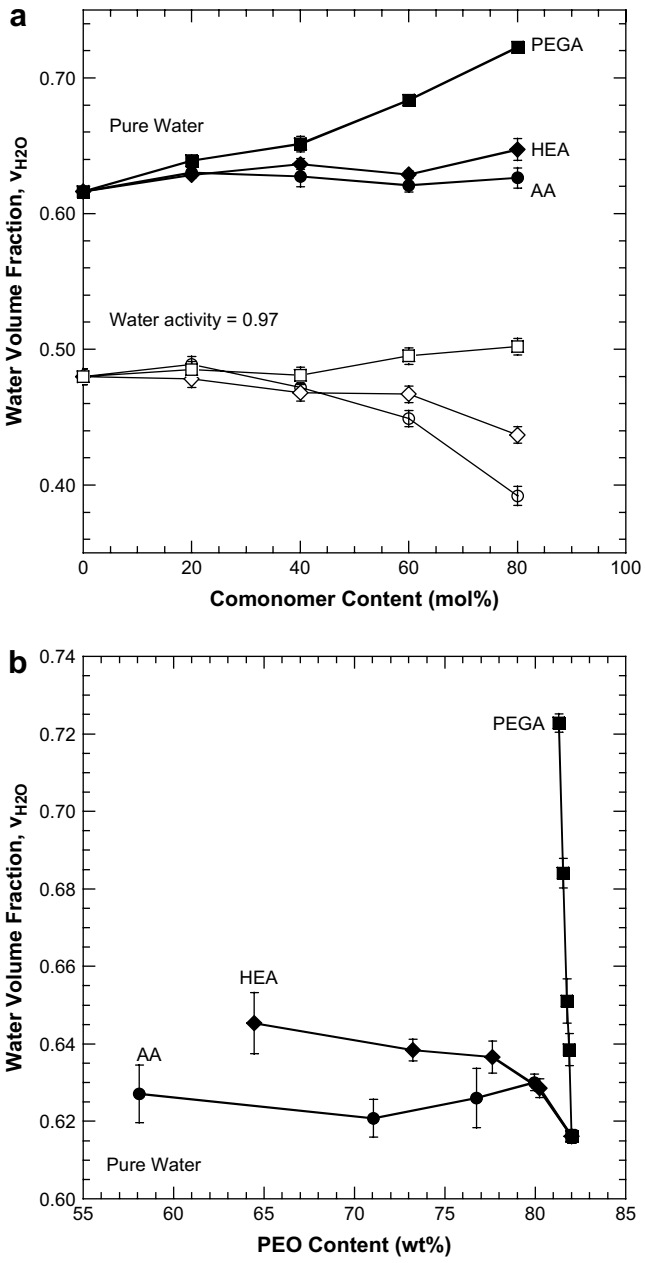

Fig. 5. Equilibrium water uptake as a function of (a) comonomer content and (b) copolymer PEO weight content. The error bars were estimated using the propagation of errors method [48].

60HEA, has water uptake between that of 60AA and 60PEGA copolymers.

Crosslink density can also influence water sorption behavior. Crosslink density decreases as monomer content increases. When all other factors are constant, decreasing crosslink density typically increases water uptake by giving the polymer network more mobility and freedom to swell [41]. However, even in the absence of crosslinks, swelling will only occur up to the solubility limit of water in the copolymer. In this regard, the PEO content of the copolymers might also influence water uptake because water has an affinity for EO units [7]. Even high molecular weight PEO is soluble in water at room temperature [42]. Fig. 5b presents the sorbed water volume fraction as a function of PEO weight percent in each copolymer. PEGDA and PEGA are both approximately 82 wt% PEO, so PEO content remains constant for this series. Therefore, the increase in water volume fraction in PEGA copolymers can be solely attributed to the decrease in crosslink density with increasing PEGA content. Conversely, AA does not contain any PEO, and HEA is 38 wt% PEO, so in addition to changing the crosslink density, the chemistry changes significantly as comonomer content increases (cf., Table 1). However, AA and HEA copolymer water volume fractions remain relatively constant over a range of chemical compositions and crosslink densities, indicating that the compositional changes appear to offset the effect of crosslink density on water volume fraction. One possibility is physical crosslinking, induced by the increased propensity of HEA and AA to participate in hydrogen bonding [22]. This physical crosslinking would restrain copolymer swelling, counterbalancing the effect of decreased chemical crosslinking.

Water permeability was determined as a function of copolymer composition and pressure. An example of the influence of pressure on the water permeability of several samples is presented in Fig. 6. For all of the samples considered, water permeability is independent of pressure. As Fig. 7 shows, trends in water permeability with respect to comonomer content are similar to trends in water sorption. That is, PEGA copolymers have the highest water permeability and exhibit increasing permeability with increasing PEGA content, while AA and HEA copolymer permeabilities are not strong functions of copolymer composition. The same arguments used to explain water sorption behavior can presumably be extended to explain water permeation behavior: decreasing crosslink density can increase water permeability at constant PEO content, and other factors, such as hydrogen bonding and changes in the chemical structure of the copolymers, counteract the effect of changing crosslink density as comonomer content is increased. The water permeability of 80AA is not reported in Fig. 7 because the sample is phase-separated, meaning that the sample is macroporous, and transport does not necessarily occur in the same manner as it does in the non-phase-separated samples, which are presumed to transport water via solution-diffusion [43]. Water permeability for 80AA is in excess of 100 L μm/(m^2 h bar), which is

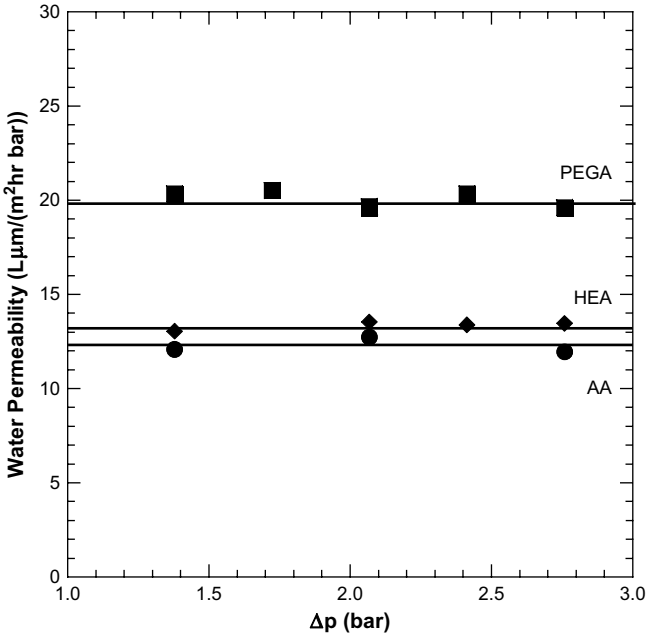

Fig. 6. Representative plot of water permeability as a function of applied transmembrane pressure. These samples were prepared with 60 mol% of the indicated comonomer (PEGA, HEA, or AA) and 40 mol% PEGDA.

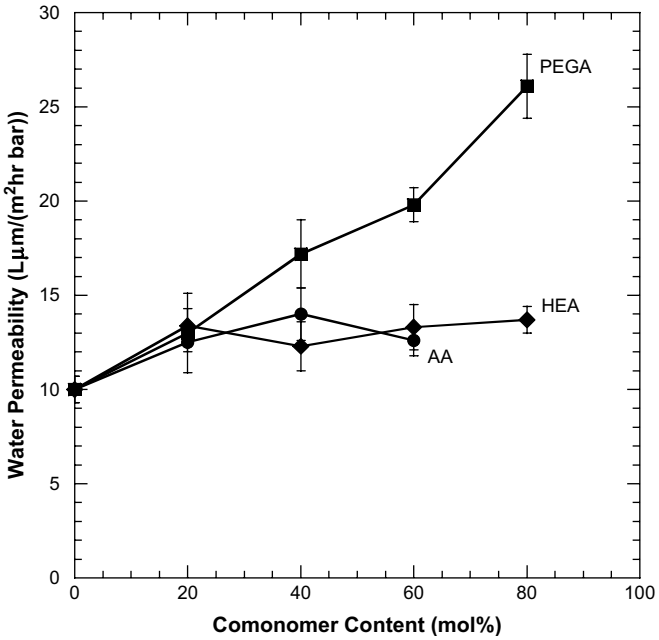

Fig. 7. Water permeability as a function of copolymer composition.

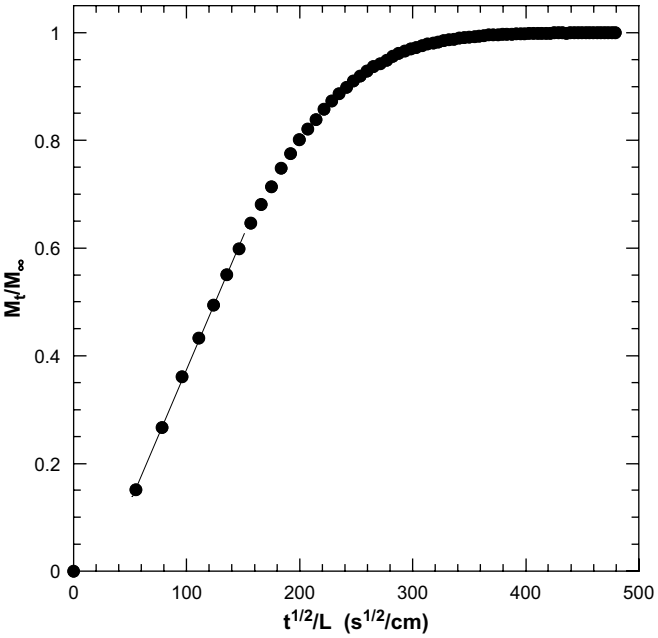

Fig. 9. Example salt desorption curve used to calculate NaCl diffusion coefficient in a hydrogel. The solid line represents the data fit to Eq. (6). The sample shown here is 40PEGA. Sample thickness, *l*, was 0.04 cm, and the resulting NaCl diffusion coefficient, calculated using Eq. (6), was $4.7 \pm 0.2 \times 10^{-6}$ cm^2/s at 25 °C.

significantly higher than that of any other sample considered in this study.

Fig. 8 presents a correlation of water permeability with water volume fraction. In general, higher sorbed water content correlates with higher hydrogel water permeability, regardless of chemical composition. This behavior is consistent with that of other hydrogel materials [5,44].

3.4. Salt transport properties

Fig. 9 presents a representative NaCl desorption curve from the kinetic desorption experiments described earlier. The NaCl desorption behavior is largely consistent with that expected from Fickian diffusion models of solute release from a film of uniform thickness [29]. A short induction period was observed in many cases, indicated by the non-linear relationship between mass uptake and the square root of time at the beginning of the experiment shown in Fig. 9. Typically, this induction behavior is attributed to boundary layer effects, before the desorbing solution concentration becomes relatively uniform [45]. In this study, the data analysis to calculate salt diffusion coefficients was conducted using data unaffected by this phenomenon. The NaCl diffusion coefficient, D_s, for each copolymer was calculated from the slope of the linear portion of the desorption curve using Eq. (6). The solid line through the data points in Fig. 9 represents the fit of Eq. (6) to this particular data set.

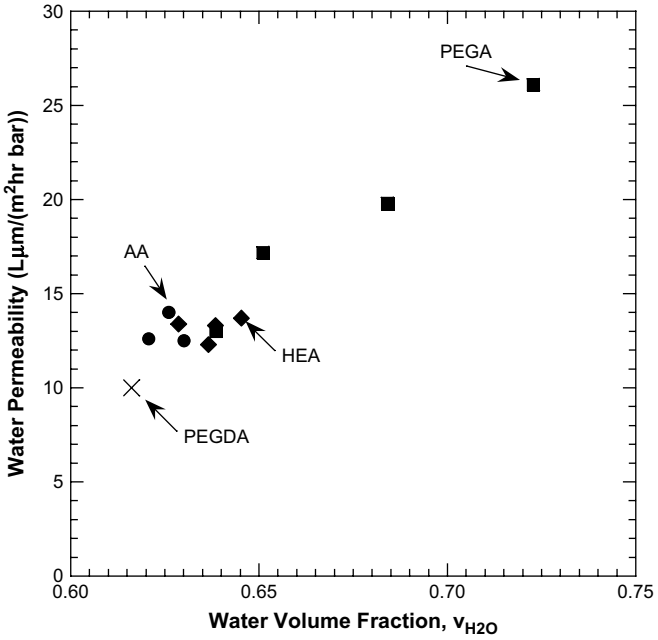

Fig. 8. Water permeability as a function of equilibrium water uptake in AA/PEGDA (●), HEA/PEGDA (◆), and PEGA/PEGDA (■) copolymers as well as in PEGDA (×).

The salt diffusion coefficients are presented as a function of polymer composition in Fig. 10a. NaCl diffusivity does not change significantly with AA or HEA content, but it increases slightly with increasing PEGA content. The difference in diffusivity between most of the copolymers is not significant, except for the 80 mol% copolymers, where the salt diffusion coefficient of 80PEGA is larger than that of 80AA. The diffusivity of NaCl in pure water at 25 °C is approximately 1.6×10^{-5} cm^2/s [46]. All of the salt diffusion coefficients in the hydrogel films are below this value, which is reasonable. Also, Yasuda et al. reported NaCl diffusion coefficients through hydrogels of different chemistries, but similar water uptake values to the materials considered in this study. Water uptake for Yasuda's materials ranged from 0.55 to 0.70 vol fraction, and their diffusion coefficients ranged from 1.8 to 8.8×10^{-6} cm^2/s [28], similar to the values obtained in this study.

NaCl partition coefficients, K_s, were also determined from the desorption measurements, and the results are presented in Fig. 10b. Trends in K_s as a function of comonomer content are reminiscent of the trends in water sorption for these materials. Like their water sorption behavior, AA and HEA copolymers show relatively little change in NaCl uptake with increasing comonomer content. However, PEGA copolymers show salt solubility, K_s, increasing with

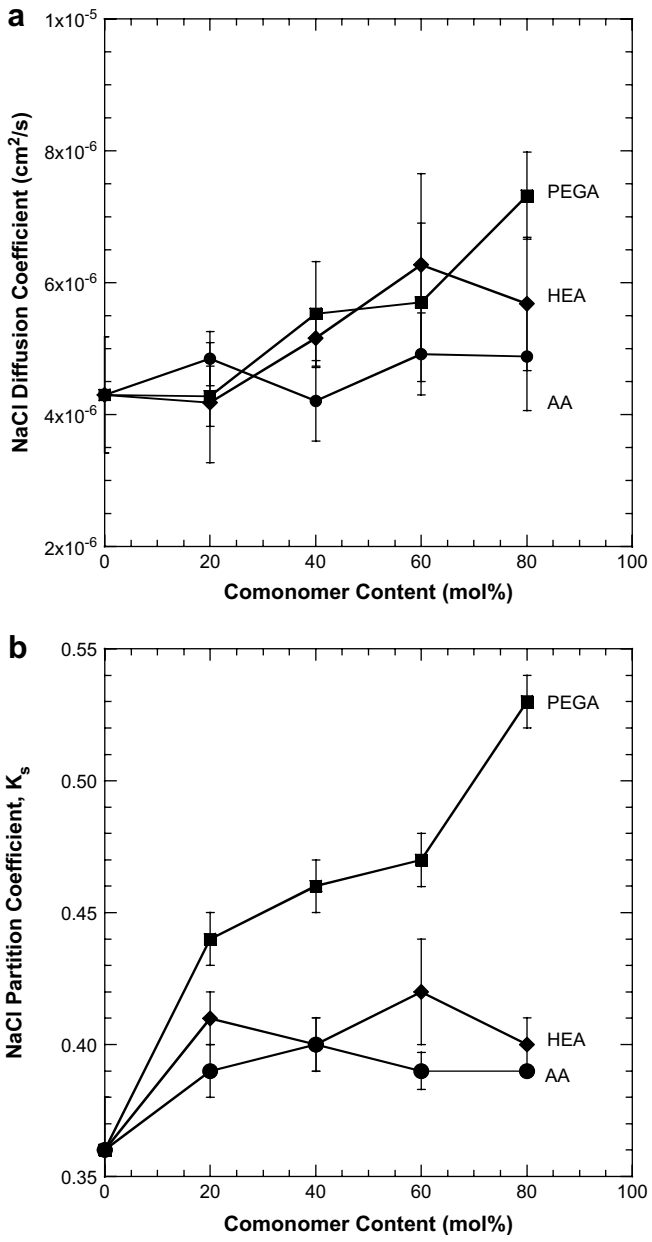

Fig. 10. (a) Diffusion and (b) partition coefficients of NaCl in hydrogel copolymers as a function of composition at 25 °C.

increasing comonomer content, similar to its water sorption behavior. These results are reasonable since the amount of salt sorbed by a hydrogel polymer network can, in some cases, be proportional to water uptake [28].

The partition coefficient data were compared to the model proposed by Yasuda et al. [28]:

$$K_s = K_{polymer}\nu_{polymer} + K_{H_2O}\nu_{H_2O} \quad (9)$$

where K_s is the measured NaCl solubility coefficient, $K_{polymer}$ and K_{H_2O} are the partition coefficients of the polymer and water, respectively, and $\nu_{polymer}$ and ν_{H_2O} are the volume fractions of polymer and water, respectively, in the swollen polymer. If NaCl is not sorbed by the polymer itself, then $K_{polymer}$ is zero. Also, K_{H_2O} is, by definition, one. Consequently, Eq. (9) reduces to [28]:

$$K_s = \nu_{H_2O} \quad (10)$$

where, in this case, ν_{H_2O} is the water volume fraction measured at a water activity of 0.97. As shown in Fig. 11, the measured partition coefficients are near or below the line given by Eq. (10), so the concentration of salt dissolved in most of the hydrogels is slightly less than predicted by the simple model outlined above. Thus, the majority of these hydrogels acts to exclude some salt from their network. These results indicate that the materials exhibit some solubility selectivity for water over NaCl, which would be useful if such materials were used as coatings for desalination membranes. Salt solubility data from Yasuda et al. for materials of similar water uptake values are similar to the data obtained in this study [28].

Using the measured D_s and K_s values, NaCl permeability coefficients were calculated according to Eq. (7). The results are presented in Fig. 12a. In the same manner as both the salt uptake and diffusion behavior, AA and HEA copolymer NaCl permeabilities are relatively constant for all comonomer contents, but PEGA copolymer NaCl permeability increases with increasing comonomer content.

Yasuda et al. developed the following model, based on free volume theory, to correlate salt permeability with water uptake [28]:

$$P_s = A\exp\left(\frac{B}{\nu_{H_2O}}\right) \quad (11)$$

where P_s is the salt permeability, and A and B are constants. Fig. 12b presents the salt permeability data from this study along with selected data from Yasuda et al. plotted as a function of inverse water uptake. The materials presented from the work of Yasuda et al. are hydrogels made from hydroxyethyl methacrylate, methyl methacrylate and glycerol methacrylate, or hydroxypropyl methacrylate and glycerol methacrylate. These materials are similar to those studied here and are considered to be standard hydrogel materials [6]. As Fig. 12b shows, the data from this study are in reasonable agreement with the literature data. Given the short range in water uptake over which the data from this study falls, the

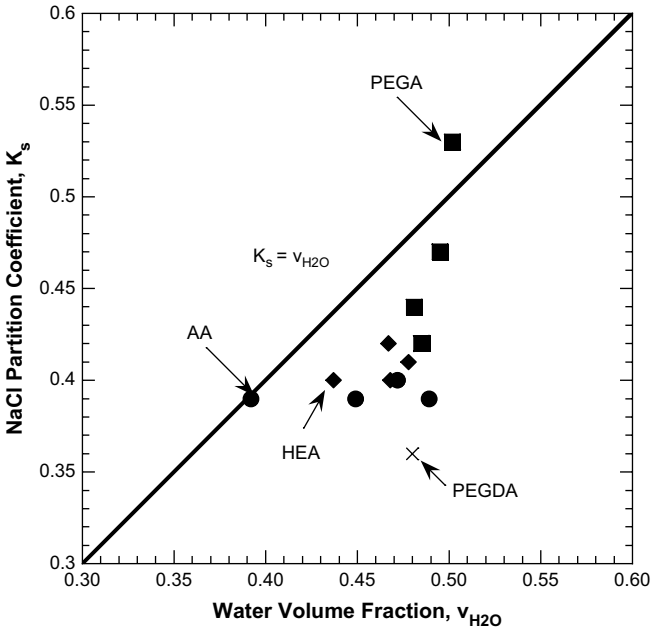

Fig. 11. Correlation between NaCl partition coefficients and polymer water volume fractions in AA/PEGDA (●), HEA/PEGDA (◆), and PEGA/PEGDA (■) copolymers as well as in PEGDA (×). Water volume fractions are those measured at water activity equal to 0.97.

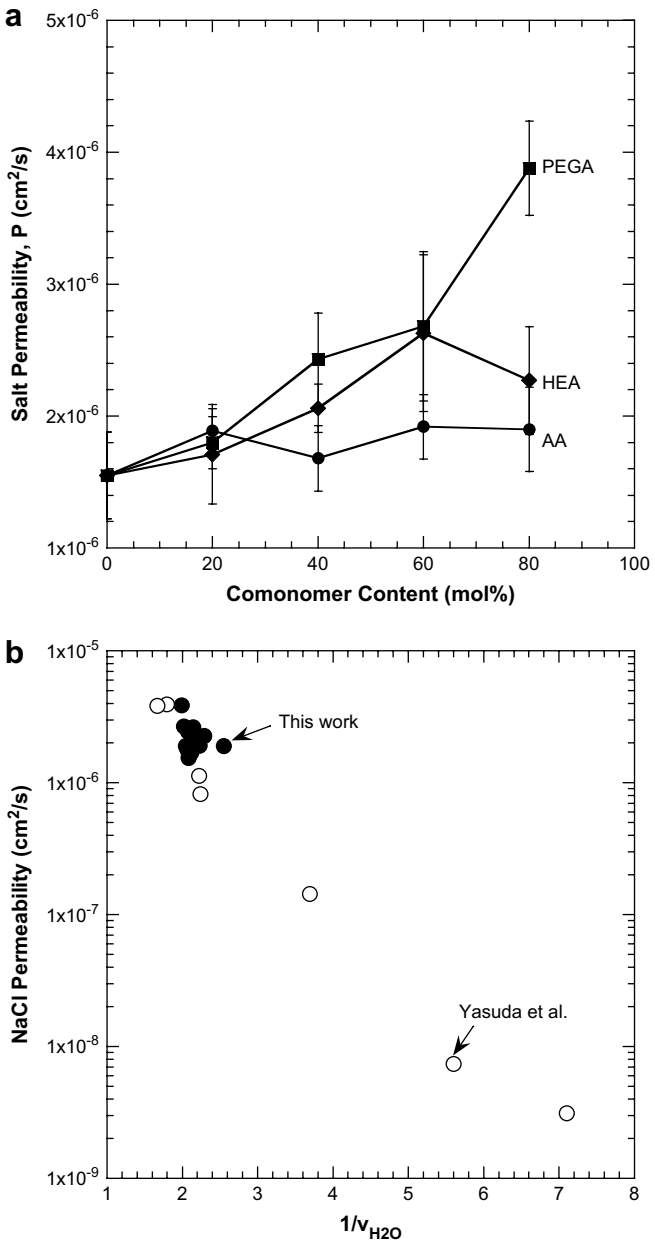

Fig. 12. NaCl permeability through hydrogels as a function of (a) copolymer composition and (b) inverse water sorption using water uptake values at water activity equal to 0.97 [44].

materials here exhibit little change in free volume with changes in copolymer composition.

3.5. Contact angle measurements

Contact angles were measured using a pendant drop technique with the copolymer films immersed in DI water. *n*-Decane was used as the probe liquid. The reported angle was measured through the aqueous phase, so angles of 90° and greater correspond to hydrophobic surfaces, and angles less than 90° correspond to hydrophilic surfaces [47]. The data are shown in Table 2. All of the contact angle values are well below 90°, indicating that these copolymers have hydrophilic surfaces. This surface hydrophilicity may assist the hydrogels in their ability to act as fouling-resistant coatings for separation of oily wastewater [5]. Despite significant differences in water sorption and water permeability among the copolymers, the contact angle values are not very sensitive to copolymer content or monomer type. However, contact angle measurements are best used to determine qualitatively if a surface is hydrophilic or hydrophobic; they typically do not afford the resolution required to detect subtle changes in surface chemistries [47].

Table 2
Oil-in-water pendant drop contact angles of hydrogel films.

Sample	Contact angle (°)
PEGDA	49 ± 2
20AA	56 ± 4
40AA	62 ± 7
60AA	54 ± 4
80AA	32 ± 3
20HEA	46 ± 3
40HEA	56 ± 8
60HEA	51 ± 1
80HEA	49 ± 4
20PEGA	48 ± 1
40PEGA	40 ± 3
60PEGA	37 ± 3
80PEGA	44 ± 4

4. Conclusions

Three series of PEG-based hydrogel copolymers were synthesized and characterized. The hydrogels sorb large amounts of water and have high water permeability. Decreasing crosslink density significantly increases water sorption and permeability at fixed PEO content, but changing chemical composition appears to offset the effect of changing crosslink density on water sorption and permeability. NaCl transport behavior follows similar trends to water transport in the hydrogels; low water uptake accompanies low salt uptake, and copolymers with high water permeability also have high NaCl permeability. Most of the hydrogels show some solubility selectivity for water over salt. Contact angle measurements indicate that all of the copolymers have hydrophilic surfaces.

Acknowledgements

The authors gratefully acknowledge partial support of this work by the U.S. Department of Energy (DOE) under DE-FC26-04NT15547, by the Office of Naval Research (ONR) under 140510771 and 140510158, and by the National Science Foundation (NSF) under CBET-0553957. However, any opinions, findings, conclusions, or recommendations expressed herein are those of the authors and do not necessarily reflect the views of the DOE, ONR or NSF.

References

[1] Service RF. Science 2006;313:1088–90.
[2] Veil JA, Puder MG, Elcock D, Redweik RJ. A white paper describing produced water from production of crude oil, natural gas, and coal bed methane. U.S. Department of Energy: National Energy Technology Laboratory; 2004.
[3] Sagle AC, Freeman BD. In: Arroyo JA, editor. The future of desalination in texas, vol. II. Texas Water Development Board; 2004. p. 137–53.
[4] Freeman BD, Pinnau I. In: Pinnau I, Freeman BD, editors. Advanced materials for membrane separations, vol. 876. Washington, DC: American Chemical Society; 2004. p. 1–23.
[5] Ju H, McCloskey BD, Sagle AC, Wu YH, Kusuma V, Freeman BD. J Membr Sci 2008;307:260–7.
[6] Peppas NA, Hilt ZH, Khademhosseini A, Langer R. Adv Mater 2006;18:1345–60.
[7] Graham NB. In: Peppas NA, editor. Hydrogels in medicine and pharmacy. Polymers, vol. II. Boca Raton: CRC Press; 1987. p. 95–113.
[8] Kelly ST, Zydney AL. J Membr Sci 1995;107:115–27.
[9] Dalsin J, Lin L, Tosatti S, Voros J, Textor M, Messersmith PB. Langmuir 2005;21:640–6.

[10] Kingshott P, Thissen H, Griesser HJ. Biomaterials 2002;23:2043–56.
[11] Lin H, Kai T, Freeman BD, Kalakkunnath S, Kalika DS. Macromolecules 2005;38:8381–93.
[12] Lin H, Van Wagner E, Swinnea JS, Freeman BD, Pas SJ, Hill AJ, et al. J Membr Sci 2006;276:145–61.
[13] Armarego WLF, Chai CLL. Purification of laboratory chemicals. 5th ed. Boston: Butterworth-Heinemann; 2003. p. 95.
[14] am Ende MT, Peppas NA. Pharm Res 1995;12:2030–5.
[15] Lee YM, Shim JK. J Appl Polym Sci 1996;61:1245–50.
[16] Ravi N, Mitra A, Hamilton P, Horkay F. J Polym Sci Part B Polym Phys 2002;40:2677–84.
[17] Krongauz VV, Chawla CP, Dupre J. In: Belfield KD, Crivello JV, editors. Photoinitiated polymerization, vol. 847. Washington, DC: American Chemical Society; 2003. p. 165–75.
[18] Dietz JE, Elliott BJ, Peppas NA. Macromolecules 1995;28:5163–6.
[19] Cramer NB, Bowman CN. J Polym Sci Part A Polym Chem 2001;39:3311–9.
[20] McCrum NG, Buckley CP, Bucknall CB. Principles of polymer engineering. Oxford: Oxford University Press; 2003.
[21] Cruise GM, Scharp DS, Hubbell JA. Biomaterials 1998;19:1287–94.
[22] Thomas JB, Tingsanchali JH, Rosales AM, Creecy CM, McGinty JW, Peppas NA. Polymer 2007;48:5042–8.
[23] Peppas NA, Barr-Howell BD. In: Peppas NA, editor. Hydrogels in medicine and pharmacy. Fundamentals, vol. I. Boca Raton: CRC; 1986. p. 27–56.
[24] Standard practice for maintaining constant relative humidity by means of aqueous solutions. ASTM E104-02; 2002.
[25] Clarke ECW, Glew DN. J Phys Chem Ref Data 1985;14:489–610.
[26] Optics and optical instruments: contact lenses – determination of thickness. Part II: hydrogel contact lenses. ISO 9339-2; 1998.
[27] Nagai K, Tanaka S, Hirata Y, Nakagawa T, Arnold ME, Freeman BD, et al. Polymer 2001;42:9941–8.
[28] Yasuda H, Lamaze CE, Ikenberry LD. Makromol Chem 1968;118:19–35.
[29] Bird RB, Stewart WE, Lightfoot EN. Transport phenomena. 2nd ed. New York: John Wiley & Sons, Inc.; 2002.
[30] Okay O. Prog Polym Sci 2000;25:711–79.
[31] Stevens MP. Polymer chemistry: an introduction. New York: Oxford University Press; 1999. p. 70–4.
[32] Kim GK, Aguilar-Vega M, Paul DR. J Polym Sci Part B Polym Phys 1992; 30:1131–42.
[33] Muruganandam N, Paul DR. J Polym Sci Part B Polym Phys 1987;25:2315–29.
[34] Coleman MM, Graf JF, Painter PC. Specific interactions and the miscibility of polymer blends. Lancaster: Technomic Publishing Company, Inc.; 1991.
[35] Jo WH, Cruz CA, Paul DR. J Polym Sci Part B Polym Phys 1989;27:1057–76.
[36] Brandrup J, Immergut EH, Grulke EA. Polymer handbook. 4th ed. New York: John Wiley & Sons, Inc.; 1999.
[37] Ellis B, editor. Polymers: a property database. Internet version. Boca Raton FL: Taylor and Francis; 2000.
[38] Pissis P, Kyritsis A, Daoukaki D. J Mol Struct 1999;479:163–75.
[39] Borns MA, Kalakkunnath S, Kalika DS, Kusuma V, Freeman BD. Polymer 2007;48:7316–28.
[40] Barrer RM. In: Crank J, Park GS, editors. Diffusion in polymers. New York: Academic Press; 1968. p. 165–219.
[41] Bajpai SK, Singh S. React Funct Polym 2006;66:431–40.
[42] Ashbaugh HS, Paulaitis ME. Ind Eng Chem Res 2006;45:5531–7.
[43] Paul DR. J Membr Sci 2004;241:371–86.
[44] Yasuda H, Lamaze CE, Peterlin A. J Polym Sci A-2 1971;9:1117–31.
[45] Crank J, Park GS. In: Crank J, Park GS, editors. Diffusion in polymers. New York: Academic Press, Inc.; 1968. p. 1–40.
[46] Fell CJD, Hutchinson HP. J Chem Eng Data 1971;16:427–9.
[47] Adamson AW, Gast AP. Physical chemistry of surfaces. 6th ed. New York: John Wiley & Sons, Inc.; 1997.
[48] Bevington PR, Robinson DK. Data reduction and error analysis for the physical sciences. 2nd ed. New York: McGraw-Hill, Inc.; 1992.